are frequently seen in patients with *RUNX1* mutations,[40] may result at least partly in the *BMI1* overexpression. Furthermore, many gene mutations have been identified in MDS patients, including PRC2 complex proteins, and some of them showed positive associations with *RUNX1* mutations.[41] Our next investigation is to clarify the effects of both expression levels and mutations of PRC2 proteins in patients with RUNX1 mutations. There is a possibility that these gene expression patterns and mutations may act to elevate the *BMI1* expression level.

BMI1 is well-known to be essential for self-renewal of hematopoietic stem cells,[42-44] in part via repression of genes involved in senescence,[45] and self-renewal of hematopoietic stem cells is enhanced by BMI1 expression in both mouse and human.[35,46] Our results showed that overexpression of BMI1 itself in human $CD34^+$ cells or a mouse BMT model does not appear to have MDS-genic potential, as reported previously.[35,46] When the $CD34^+$ cells were double-transduced simultaneously with D171N and BMI1, the cells could proliferate with differentiation and dysplasia. Co-transduction of D171N and BMI1 into BM cells resulted in faster induction of MDS/AML in BMT mice. It is suggested that BMI1 overexpression may act as one of the partner abnormalities collaborating with master gene mutations for MDS-genesis. BMI1 affects *INK4A/ARF* expression, which has been sufficiently elucidated, involved in the leukemic phenotype. A previous report that showed that BMI1 collaborates with BCR-ABL in leukemic transformation also supports this idea.[47] We confirmed that significant enrichments of BMI1 were detected on *Ink4a/Arf* promoter regions in both BMI1-transduced cells and BMI1/D171N-transduced cells, suggesting that BMI1 overexpression may help cells transform, at least in part, due to suppressing the expression of the *Ink4a/Arf* tumor suppressor gene. Although a physical association *in vivo* between BMI1 and D171N, as well as wild type RUNX1,[48] was observed, it is known that D171N mutant has lost the DNA binding ability.[12] Therefore, the mechanism by which BMI1 co-expression with D171N mutant induces proliferative effects seems to be independent of the direct physical association between RUNX1 and BMI1. Additionally, both BMI1-knockdown human $CD34^+$ cells and *Bmi1*-deficient mouse cells showed elevated levels of reactive oxygen species accumulation,[49,50] resulting in impairment of long-term expansion and apoptosis. It may be the reason why D171N-transduced human $CD34^+$ cells that showed reduced BMI1 expression could not proliferate. It may also explain the phenomenon in 32Dcl3 cells, in which BMI1 transduction seemed to rescue D171N-transduced cells from apoptosis. However, the $CD34^+$ cells transduced with D171N/BMI1 did not develop MDS/AML in NOG mice, suggesting that other factors such as *EVI1* overexpression observed in

a mouse BMT model may be still required for the development of MDS/AML in NOG mice.

Germline mutations of *RUNX1* have been shown to occur in FPD/AML.[1,2] FPD/AML is regarded as familial MDS,[3] and the molecular mechanisms by which RUNX1 mutations promote the development of hematopoietic malignancies seem to be identical in both MDS and FPD/AML patients. Because decades-long asymptomatic latency period do occur in patients with FPD/AML, it appears that RUNX1-mutated stem cells cannot promote the development of MDS without other cooperative factors. It is suspected that additional gene abnormalities occur later on in the RUNX1-mutated cells for the development of MDS. Therefore, we performed stepwise transduction of the D171N mutant followed by BMI1 into $CD34^+$ cells, which could reproduce continuous slow proliferation of a low percentage of blastoid cells, reflecting the hematological features in higher-risk MDS patients. This result indicates that genetic alterations, such as EVI1 or BMI1 overexpression which add proliferative advantage to cells, may occur as "second hits" after the master genetic alteration (i.e. RUNX1 mutation) that has MDS-genic potential.

In the present study, we revealed the functional significance of the RUNX1 D171N mutant in the pathogenesis of MDS using human $CD34^+$ cells. Thus, amino acid replacement type mutations in the RHD, which comprise half of the RUNX1 mutations detected in patients, are suspected to have MDS-genic potential, however, the cells with this type of mutation lack proliferation ability. This may explain bone marrow failure status, one of the phenotypes of MDS. When the mutated cells gain partner gene abnormality, i.e. *EVI1* or *BMI1* overexpression, they can acquire proliferation ability through alteration of the collaborating gene which may explain the various clinical features of patients with RUNX1 mutations. On the other hand, the other half of the RUNX1 mutants may have different biochemical functions that remain unclear, in particular, mutants that lack the C-terminal functional domain but have an intact RHD may have other effects.[4,22] Our future investigations include the elucidation and clarification of the molecular mechanisms by which each type of RUNX1 mutant promotes the development of MDS.

Acknowledgments

The authors would like to acknowledge the pregnant women, nursing staff, and Dr. Hanioka at Yamashita Clinic for providing cord blood. We are grateful to Ryoko Matsumoto-Yamaguchi provided excellent technical support in carrying out these experiments.

This work was supported in part by Grants-in-Aid for Scientific Research from the Ministry of Education, Culture, Sports, Science and Technology of Japan grants; Hiroshima University grants; Japan Leukaemia Research Fund and Radiation Effects Association grant. This work was carried out in part at the Analysis Center of Life Science, Hiroshima University.

Authorship Contributions

Y.H. designed the research, performed experiments and wrote the manuscript; D.I. and Y.D. performed experiments and prepared the manuscript; J.I., N.D., H.Matsui, T.Y., H.Matsushita and G.S. collected the data; K.A., A.I. and T.K. supervised the project and discussed the results; and H.H. conceived and designed the research, collected and interpreted the data, and revised the manuscript.

Disclosure of Conflicts of Interest

The authors declare that no conflict of interest exists.

References

1. Song WJ, Sullivan MG, Legare RD, et al. Haploinsufficiency of CBFA2 causes familial thrombocytopenia with propensity to develop acute myelogenous leukaemia. *Nat Genet.* 1999;23(2):166-175.

2. Osato M. Point mutations in the RUNX1/AML1 gene: another actor in RUNX leukemia. *Oncogene.* 2004;23(24):4284-4296.

3. Liew E, Owen C. Familial myelodysplastic syndromes: a review of the literature. *Haematologica.* 2011;96(10):1536-1542.

4. Harada H, Harada Y, Niimi H, Kyo T, Kimura A, Inaba T. High incidence of somatic mutations in the AML1/RUNX1 gene in myelodysplastic syndrome and low blast percentage myeloid leukemia with myelodysplasia. *Blood.* 2004;103(6):2316-2324.

5. Preudhomme C, Warot-Loze D, Roumier C, et al. High incidence of biallelic point mutations in the Runt domain of the AML1/PEBP2 alpha B gene in Mo acute myeloid leukemia and in myeloid malignancies with acquired trisomy 21. *Blood.* 2000;96(8):2862-2869.

6. Dicker F, Haferlach C, Kern W, Haferlach T, Schnittger S. Trisomy 13 is strongly associated with AML1/RUNX1 mutations and increased FLT3 expression in acute myeloid leukemia. *Blood.* 2007;110(4):1308-1316.

7. Silva FPG, Swagemakers SMA, Erpelinck-Verschueren C, et al. Gene expression profiling of minimally differentiated acute myeloid leukemia: M0 is a distinct entity subdivided by RUNX1 mutation status. *Blood.* 2009;114(14):3001-3007.

8. Tang JL, Hou HA, Chen CY, et al. AML1/RUNX1 mutations in 470 adult patients with de novo acute myeloid leukemia: prognostic implication and interaction with other gene alterations. *Blood.* 2009;114(26):5352-5361.

9. Schnittger S, Dicker F, Kern W, et al. RUNX1 mutations are frequent in de novo AML with noncomplex karyotype and confer an unfavorable prognosis. *Blood.* 2011;117(8):2348-2357.

10. Kuo MC, Liang DC, Huang CF, et al. RUNX1 mutations are frequent in chronic myelomonocytic leukemia and mutations at the C-terminal region might predict acute myeloid leukemia transformation. *Leukemia.* 2009;23(8):1426-1431.

11. Ernst T, Chase A, Zoi K, et al. Transcription factor mutations in myelodysplastic/myeloproliferative neoplasms. *Haematologica.* 2010;95(9):1473-1480.

12. Harada H, Harada Y, Tanaka H, Kimura A, Inaba T. Implications of somatic mutations in the AML1 gene in radiation-associated and therapy-related myelodysplastic syndrome/acute myeloid leukemia. *Blood.* 2003;101(2):673-680.

13. Christiansen DH, Andersen MK, Pedersen-Bjergaard J. Mutations of AML1 are common in therapy-related myelodysplasia following therapy with alkylating agents and are significantly associated with deletion or loss of chromosome arm 7q and with subsequent leukemic transformation. *Blood.* 2004;104(5):1474-1481.

14. Zharlyganova D, Harada H, Harada Y, et al. High frequency of AML1/RUNX1 point mutations in radiation-associated myelodysplastic syndrome around Semipalatinsk nuclear test site. *J Radiat Res (Tokyo).* 2008;49(5):549-555.

15. Imagawa J, Harada Y, Shimomura T, et al. Clinical and genetic features of therapy-related myeloid neoplasms after chemotherapy for acute promyelocytic leukemia. *Blood.* 2010;116(26):6018-6022.

16. Ding Y, Harada Y, Imagawa J, Kimura A, Harada H. AML1/RUNX1 point mutation possibly promotes leukemic transformation in myeloproliferative neoplasms. *Blood.* 2009;114(25):5201-5205.

17. Beer PA, Delhommeau F, LeCouedic JP, et al. Two routes to leukemic transformation after a JAK2 mutation-positive myeloproliferative neoplasm. *Blood.* 2010;115(14):2891-2900.

18. Zhao LJ, Wang YY, Li G, et al. Functional features of RUNX1 mutants in acute transformation of chronic myeloid leukemia and their contribution to inducing murine full-blown leukemia. *Blood.* 2012;119(12):2873-2882.

19. Grossmann V, Kohlmann A, Zenger M, et al. A deep-sequencing study of chronic myeloid leukemia patients in blast crisis (BC-CML) detects mutations in 76.9% of cases. *Leukemia.* 2011;25(3):557-560.

20. Tahirov TH, Inoue-Bungo T, Morii H, et al. Structural analyses of DNA recognition by the AML1/Runx-1 Runt domain and its allosteric control by CBFbeta. *Cell.* 2001;104(5):755-767.

21. Bravo J, Li Z, Speck NA, Warren AJ. The leukemia-associated AML1 (Runx1)--CBF beta complex functions as a DNA-induced molecular clamp. *Nat Struct Biol.* 2001;8(4):371-378.

22. Watanabe-Okochi N, Kitaura J, Ono R, et al. AML1 mutations induced MDS and MDS/AML in a mouse BMT model. *Blood.* 2008;111(8):4297-4308.

23. Cattoglio C, Facchini G, Sartori D, et al. Hot spots of retroviral integration in human CD34+ hematopoietic cells. *Blood.* 2007;110(6):1770-1778.

24. Schwieger M, Lohler J, Fischer M, Herwig U, Tenen DG, Stocking C. A dominant-negative mutant of C/EBPalpha, associated with acute myeloid leukemias, inhibits differentiation of myeloid and erythroid progenitors of man but not mouse. *Blood.* 2004;103(7):2744-2752.

25. Xu F, Li X, Wu L, et al. Overexpression of the EZH2, RING1 and BMI1 genes is common in myelodysplastic syndromes: relation to adverse epigenetic alteration and poor prognostic scoring. *Ann Hematol.* 2011;90(6):643-653.

26. Mihara K, Chowdhury M, Nakaju N, et al. Bmi-1 is useful as a novel molecular marker for predicting progression of myelodysplastic syndrome and patient prognosis. *Blood.* 2006;107(1):305-308.

27. Mulloy JC, Cammenga J, MacKenzie KL, Berguido FJ, Moore MA, Nimer SD. The AML1-ETO fusion protein promotes the expansion of human hematopoietic stem cells. *Blood.* 2002;99(1):15-23.

28. Tonks A, Pearn L, Tonks AJ, et al. The AML1-ETO fusion gene promotes extensive self-renewal of human primary erythroid cells. *Blood.* 2003;101(2):624-632.

29. Mulloy JC, Cammenga J, Berguido FJ, et al. Maintaining the self-renewal and differentiation potential of human CD34+ hematopoietic cells using a single genetic element. *Blood.* 2003;102(13):4369-4376.

30. D'Costa J, Chaudhuri S, Civin CI, Friedman AD. CBFbeta-SMMHC slows proliferation of primary murine and human myeloid progenitors. *Leukemia.* 2005;19(6):921-929.

31. Wunderlich M, Krejci O, Wei J, Mulloy JC. Human CD34+ cells expressing the inv(16) fusion protein exhibit a myelomonocytic phenotype with greatly enhanced proliferative ability. *Blood.* 2006;108(5):1690-1697.

32. Shen SW, Dolnikov A, Passioura T, et al. Mutant N-ras preferentially drives human CD34+ hematopoietic progenitor cells into myeloid differentiation and proliferation both in vitro and in the NOD/SCID mouse. *Exp Hematol.* 2004;32(9):852-860.

33. Chou FS, Wunderlich M, Griesinger A, Mulloy JC. N-Ras(G12D) induces features of stepwise transformation in preleukemic human umbilical cord blood cultures expressing the AML1-ETO fusion gene. *Blood*. 2011;117(7):2237-2240.

34. Chung KY, Morrone G, Schuringa JJ, Wong B, Dorn DC, Moore MA. Enforced expression of an Flt3 internal tandem duplication in human CD34+ cells confers properties of self-renewal and enhanced erythropoiesis. *Blood*. 2005;105(1):77-84.

35. Rizo A, Dontje B, Vellenga E, de Haan G, Schuringa JJ. Long-term maintenance of human hematopoietic stem/progenitor cells by expression of BMI1. *Blood*. 2008;111(5):2621-2630.

36. Kato N, Kitaura J, Doki N, et al. Two types of C/EBPalpha mutations play distinct but collaborative roles in leukemogenesis: lessons from clinical data and BMT models. *Blood*. 2011;117(1):221-233.

37. Ito M, Hiramatsu H, Kobayashi K, et al. NOD/SCID/γ mouse: an excellent recipient mouse model for engraftment of human cells. *Blood*. 2002;100(9):3175-3182.

38. Tsuzuki S, Hong D, Gupta R, Matsuo K, Seto M, Enver T. Isoform-specific potentiation of stem and progenitor cell engraftment by AML1/RUNX1. *PLoS Med*. 2007;4(5):e172.

39. Motoda L, Osato M, Yamashita N, et al. Runx1 protects hematopoietic stem/progenitor cells from oncogenic insult. *Stem Cells*. 2007;25(12):2976-2986.

40. Niimi H, Harada H, Harada Y, et al. Hyperactivation of the RAS signaling pathway in myelodysplastic syndrome with AML1/RUNX1 point mutations. *Leukemia*. 2006;20(4):635-644.

41. Bejar R, Stevenson K, Abdel-Wahab O, et al. Clinical effect of point mutations in myelodysplastic syndromes. *N Engl J Med*. 2011;364(26):2496-2506.

42. van der Lugt NM, Domen J, Linders K, et al. Posterior transformation, neurological abnormalities, and severe hematopoietic defects in mice with a targeted deletion of the bmi-1 proto-oncogene. *Genes Dev*. 1994;8(7):757-769.

43. Park IK, Qian D, Kiel M, et al. Bmi-1 is required for maintenance of adult self-renewing haematopoietic stem cells. *Nature*. 2003;423(6937):302-305.

44. Lessard J, Sauvageau G. Bmi-1 determines the proliferative capacity of normal and leukaemic stem cells. *Nature*. 2003;423(6937):255-260.

45. Jacobs JJ, Kieboom K, Marino S, DePinho RA, van Lohuizen M. The oncogene and Polycomb-group gene bmi-1 regulates cell proliferation and senescence through the ink4a locus. *Nature.* 1999;397(6715):164-168.

46. Iwama A, Oguro H, Negishi M, et al. Enhanced self-renewal of hematopoietic stem cells mediated by the polycomb gene product Bmi-1. *Immunity.* 2004;21(6):843-851.

47. Rizo A, Horton SJ, Olthof S, et al. BMI1 collaborates with BCR-ABL in leukemic transformation of human CD34+ cells. *Blood.* 2010;116(22):4621-4630.

48. Yu M, Mazor T, Huang H, et al. Direct recruitment of polycomb repressive complex 1 to chromatin by core binding transcription factors. *Mol Cell.* 2012;45(3):330-343.

49. Rizo A, Olthof S, Han L, Vellenga E, de Haan G, Schuringa JJ. Repression of BMI1 in normal and leukemic human CD34(+) cells impairs self-renewal and induces apoptosis. *Blood.* 2009;114(8):1498-1505.

50. Liu J, Cao L, Chen J, et al. Bmi1 regulates mitochondrial function and the DNA damage response pathway. *Nature.* 2009;459(7245):387-392.

Table 1. Characteristics of AML mice caused by expression of D171N and BMI1

	pMYs.IG/pMYs.IN (n=3)	D171N/ pMYs.IN (n=5)	D171N/BMI1 (n=10)
WBC (/μL)	18,550 ± 1,786	129,100 ± 68,089	70,838 ± 16,353
Hb (g/dL)	14.8 ± 0.4	7.3 ± 2.5	7.7 ± 2.3
Plt ($x10^3$/μL)	291 ± 67	246 ± 80	134 ± 75
MCV (fL)	46.7 ± 0.6	53.6 ± 3.9	51.9 ± 9.3
BM count ($x10^7$ cells)	2.70 ± 0.78	7.05 ± 1.67	4.83 ± 1.14
Myeloblasts in BM (%)	1.8 ± 1.0	34.5 ± 16.0	59.6 ± 8.2
Liver weight (mg)	1,668 ± 129	2,008 ± 482	2,015 ± 527
Spleen weight (mg)	98 ± 12	605 ± 242	531 ± 185

Averages and standard deviations are shown. BM cells were isolated from both tibias and femurs.

WBC indicates white blood cell; Hb, hemoglobin; Plt, platelets; and MCV, mean corpuscular volume.

Figure Legends

Figure 1. *EVI1* overexpression collaborates with *RUNX1* mutations in human MDS. (A) *EVI1* expression levels by quantitative reverse transcription-polymerase chain reaction (qRT-PCR) in $CD34^+$ cells of clinical samples. Relative *EVI1* expression was calculated as the ratio of *EVI1* to *GAPDH* expression. RNA from normal bone marrow (BM) $CD34^+$ cells served as a control, and the RNA level was defined as one. Data are expressed as mean ± SD. L-MDS, lower-risk MDS; H-MDS, higher-risk MDS; WT, wild-type; MT, mutation. (B) White blood cell (WBC) count and clinical course of a patient with high *EVI1* expression. A 78-year-old male showed pancytopenia and blast cells in peripheral blood. Bone marrow examination showed hypocellular marrow with multilineage dysplasia and 16.5% of blast cells. Cytogenetic analysis showed 45,XY,add(3)(q?13.2),-7. He was diagnosed with RAEB-2 and received chemotherapy. However, his condition progressed to bone marrow failure after chemotherapy and repeated severe infection. Blast population continued to increase gradually. Eight months after diagnosis, his WBC count started to increase, and he died with uncontrollable blast expansion 11.5 months after diagnosis.

Figure 2. Overexpression of D171N promotes inhibition of differentiation and increase in self-renewal capacity. (A) Pictogram of pMXs.IG retroviral constructs of FLAG-tagged RUNX1 wild-type (WT) and D171N mutant (D171N). The difference in cDNA sequence of the mutant from the WT is indicated by an arrow head. LTR, long terminal repeat. (B) Human $CD34^+$ cord blood cells were transduced with the indicated vector. A typical flow cytometry profile of cells retrovirally transduced with pMXs.IG, WT or D171N shows the transduction efficiency. The GFP-positive cells shown within the gate were collected. (C) Anti-FLAG immunoblotting of sorted GFP-positive cells confirmed the expression of FLAG-tagged RUNX1 proteins. Anti-β-actin antibody was used as control. (D-H) Ten thousand cells were plated in methylcellulose culture dishes. BFU-E, burst forming unit erythroid; CFU-GM, colony forming unit-granulocyte, macrophage; GEMM, colony forming unit-granulocyte, erythroid, macrophage, megalocyte. Data are expressed as mean ± SD of 6 independent experiments and compared with control (pMXs.IG). $^*P < 0.05$, $^{**}P < 0.01$. (D) Colony numbers were counted after 14 days. (E) Photomicrographs (x40) of representative colonies found in the plates with an IX71 microscope and a DP12 camera (Olympus). (F) The cell number per colony was calculated by total GPA^+ cells / total BFU-E colonies and total $CD13^+$ cells / total CFU-GM colonies. (G) GFP^+ cells were analyzed by flow cytometry for the indicated surface markers. (H) Colony number and cell proliferation fold in CFC

replating assay. (I) LTC-IC assay in bulk was carried out in duplicate, and average number of LTC-IC per 10,000 original input cells and SD of 4 independent experiments are indicated. $^{**}P < 0.01$.

Figure 3. D171N-transduced cells lack long-term proliferation ability. Human $CD34^+$ cord blood cells were transduced with the indicated vectors and cultured in complete cytokine medium (without IL-3 and IL-6). To examine proliferation ability of each transduced cell type, the cells were sorted for GFP expression and cultured in complete cytokine medium. Four independent experiments were performed, and the error bars represent the SD. (A) Proliferation curve of GFP-positive RUNX1-transduced or control (empty vector-transduced) cells, non-sorted. (B) Growth patterns of the GFP-sorted transduced cells displayed as proliferation fold originating from one just after sorting. (C) Representative quantitative cell cycle analysis allowed the discrimination of cell subsets that were undergoing G0/G1 (a), S (b) or G2 + M (c) phases of the cell cycle, or apoptosis (d). (D) Percentage of $CD34^+$ cells was determined by flow cytometry. (E) Representative CD34/CD38 expression pattern in long-term culture. (F) Images of Wright-Giemsa stained cytospins on days 3 and 35 obtained with a BX51 microscope and a DP12 camera (Olympus); original magnification, x1000. (G) Morphological abnormalities observed in Wright-Giemsa stained cytospins of the D171N cells on day 35 in culture, myeloid, erythroid, and megakaryocytic cells with dysplasia are indicated by blue, pink, and green arrows, respectively, as captured with a BX51 microscope and a DP12 camera (Olympus); original magnification, x1000.

Figure 4. BMI1 expression pattern in human $CD34^+$ cells and enforced BMI1 expression in human $CD34^+$ cells. (A) BMI1 expression levels in $CD34^+$ cells of clinical samples. Relative BMI1 expression was measured by triplicated qRT-PCR and calculated as the ratio of BMI1 to GAPDH expression. Data are also expressed as mean ± SD of each patient group. $^{**}P < 0.01$. (B) BMI1 expression in transduced $CD34^+$ cells was confirmed by qRT-PCR. $CD34^+$ cells were re-purified from GFP-positive sorted cells after 5 and 40 days of culture in complete cytokine medium. Bar chart represents the mean ± SD of 3 independent experiments. RNA from pMXs.IG-transduced cells on day 5 served as a control, and the RNA level was defined as one. $^{*}P < 0.05$, $^{**}P < 0.01$. (C) pMXs.IRES-DsRed-Express (pMXs.IR) retroviral construct for the expression of BMI1. (D) Representative flow cytometry profile of cells retrovirally transduced with pMXs.IR or BMI1 shows the transduction efficiency. The $DsRed^+$ cells shown within the gate were collected. (E) Expression of BMI1 was confirmed by Western blotting using anti-Bmi1 antibody. Anti-β-actin antibody was used as control. (F) Human $CD34^+$ cells transduced with the indicated vector and sorted for DsRed expression were analyzed by CFC replating assay. Ten

thousand cells were plated in methylcellulose culture dishes. Data are expressed as mean ± SD of 3 independent experiments. (G) Growth pattern of the transduced cells cultured in complete cytokine medium displayed as proliferation fold originating from 10^0 just after sorting. The error bars represent the SD from 4 independent experiments. (H) The expression pattern of surface markers as shown by a typical flow cytometry profile, and Wright-Giemsa stained cytospins of the $DsRed^+$ cells on day 42 culture in complete cytokine medium as captured with a BX51 microscope and a DP12 camera (Olympus); original magnification, x1000.

Figure 5. The effect of double expression of D171N and BMI1. (A-C) IL-3-dependent 32Dcl3 cells were stably transduced with pMYs.IP/IB, pMYs.IP/BMI1, D171N/pMYs.IB or D171N/BMI1. Before the assay for proliferation and apoptosis, the transduced 32Dcl3 cells were subjected to drug selection with 1μg/mL puromycin and 10 μg/mL blasticidin. (A) G-CSF–induced differentiation assay in indicated 32Dcl3 transfectants. Surface expression of CD11b after incubation for 6 days in the presence of 1 ng/mL IL-3 (red histograms) or 50 ng/mL G-CSF (blue histograms) was analyzed by flow cytometry. The result of control staining is shown as a filled histogram. Data are representative of two independent experiments. The cells cultured with G-CSF for 6 days were assessed by Giemsa staining. Images were obtained with a BX51 microscope and a DP12 camera (Olympus); objective lens, UplanFI (Olympus); original magnification x1000. (B) Growth curve of the transduced 32Dcl3 cells cultured in the presence of 1 ng/mL of IL-3. Data are expressed as mean ± SD of 3 independent experiments. (C) Annexin V positivity in the transduced 32Dcl3 cells cultured without IL-3. Data are expressed as mean ± SD of 3 independent experiments. (D-G) Human $CD34^+$ cells were precultured for 3-4 days in expansion medium and transduced with both GFP-tagged D171N and DsRed-tagged BMI1. After 3-4 days, $GFP^+/DsRed^+$ cells were purified by sorting. The cells were cultured in methylcellulose or long-term culture medium. (D) Expression of BMI1 and RUNX1-D171N were confirmed by Western blotting using anti-Bmi1 and anti-FLAG M2 antibodies, respectively. Anti-β-actin antibody was used as control. (E) Double-transduced cells were analyzed by CFC replating assay. Data are expressed as mean ± SD from 4 independent experiments. (F) LTC-IC assay in bulk and limiting dilution was carried out. (G) Growth patterns of the transduced cells cultured in long-term culture medium displayed as proliferation fold. The error bars represent the SD from 4 independent experiments. The growth profiles of all cells with double transduction of GFP (empty or D171N) and DsRed (empty or BMI1) vectors are shown. (H) Cell cycle analysis and the expression pattern of surface markers as shown by a typical flow cytometry profile, and

Wright-Giemsa stained cytospins of D171N- and D171N/BMI1-transduced cells on day 42 as captured with a BX51 microscope and a DP12 camera (Olympus); original magnification, x1000. (I) *INK4A/ARF* (*p16/p14*) expression levels in D171N- and D171N/BMI1-transduced cells on day 42. Relative gene expression was measured by qRT-PCR performed in triplicate and calculated as the ratio of *INK4A/ARF* to *GAPDH* expression.

Figure 6. The effect of double expression of D171N and BMI1 in a mouse BMT model. (A) Kaplan-Meier analysis of the survival of mice that received transplants of BM cells transduced with pMYs.IG/BMI1 (n=12, green line), D171N/pMYs.IN (n=11, red line) or D171N/BMI1 (n=12, blue line). *P* values were calculated using log-rank test. (B) Expression of RUNX1-D171N and BMI1 in BM cells derived from the BMT mice transduced with pMYs.IG/IN (lane 1), D171N/pMYs.IN (lanes 2, 3) or D171N/BMI1 (lanes 4-8). Cell lysates were immunoblotted with anti-Bmi-1, anti-FLAG M2 or anti-tubulin antibody as control. Data are representative of 3 independent experiments. (C) Macroscopic findings of sacrificed mice transplanted with BM cells transduced with the indicated construct. A representative photograph is shown. Mice with D171N/pMYs.IN or D171N/BMI1 died of MDS/AML with marked splenomegaly (right two panels), although mice with pMYs.IG/IN or pMYs.IG/BMI1 remained healthy without any organomegaly 8 months after BMT (left two panels). (D) Cytospin preparations of BM and spleen cells derived from indicated mice were stained with Giemsa. A representative photograph is shown. Images were obtained with a BX51 microscope and a DP12 camera (Olympus); objective lens, UplanFI (Olympus); original magnification x1000. (E) Flow cytometric analysis of BM cells derived from each transduced mouse. In pMYs.IG/IN and pMYs.IG/BMI1, apparently healthy mice were sacrificed for analysis of BM cells 8 months after BMT. The dot plots show staining for NGFR, Gr-1, CD11b, B220 or c-kit as detected with phycoerythrin versus GFP. (F) Histopathologic findings of spleen and liver from mice that died of MDS/AML in the indicated BMT model, as shown by hematoxylin and eosin staining. Images were obtained with a BX51 microscope and a DP12 camera (Olympus) with an UplanFL objective lens (Olympus), and are shown at an original magnification x400. (G) *Ink4a/Arf* (*p16/p19*) expression levels in BM cells of mice. Relative *p16/p19* expression was measured by qRT-PCR performed in triplicate and calculated as the ratio of *p16/p19* to *Gapdh* expression. (H) *Evi1* expression levels in BM cells of mice. Relative *Evi1* expression was measured by qRT-PCR performed in triplicate and calculated as the ratio of *Evi1* to *Gapdh* expression. RNA from pMYs.IG/pMYs.IN mice served as a control, and the RNA level was defined as one.

Figure 7. Stepwise transduction of the D171N mutant followed by BMI1 in human CD34$^+$ cells. (A) Human CD34$^+$ cells were precultured for 3 to 4 days in expansion medium and transduced with GFP-tagged D171N-mutant. After 3 or 4 days, GFP$^+$ cells were sorted and cultured in long-term culture medium for 28 days. Then, CD34$^+$ cells were re-selected by the CD34 MicroBead Kit again, and transduced with DsRed-tagged BMI1. We also transduced the DsRed vector as a control. Finally, 35 days after the D171N transduction, GFP$^+$/DsRed$^+$ cells were sorted and cultured in methylcellulose or long-term culture medium. (B) CFC replating assay in 3 independent experiments. (C) Representative flow cytometry analyses of the first colonies. (D) Proliferation fold in 3 independent experiments. Day 0 was the day of the second (DsRed vectors) transduction. (E) Flow cytometric analysis for CD34 expression, and Wright-Giemsa stained cytospins on day 39 as captured with a BX51 microscope and a DP12 camera (Olympus) at x400 and x1000 original magnifications.

Figure 1

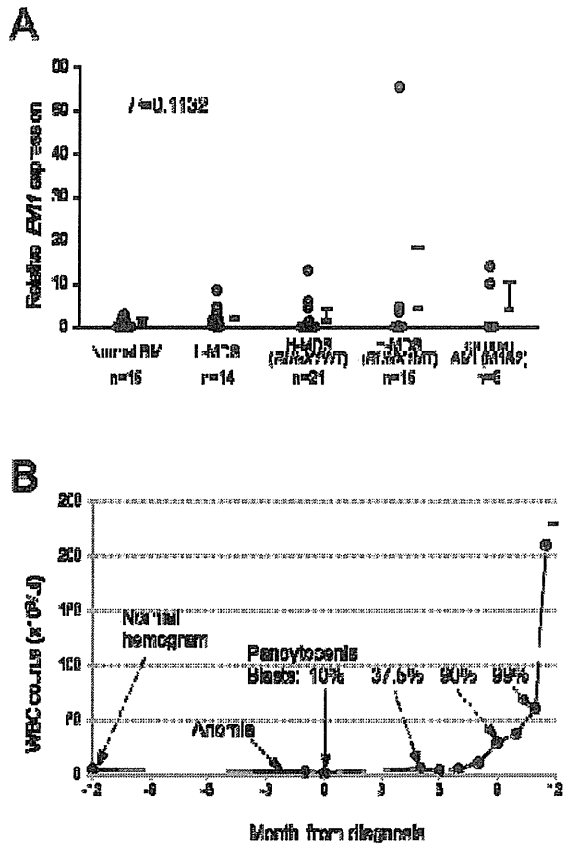

Figure 2

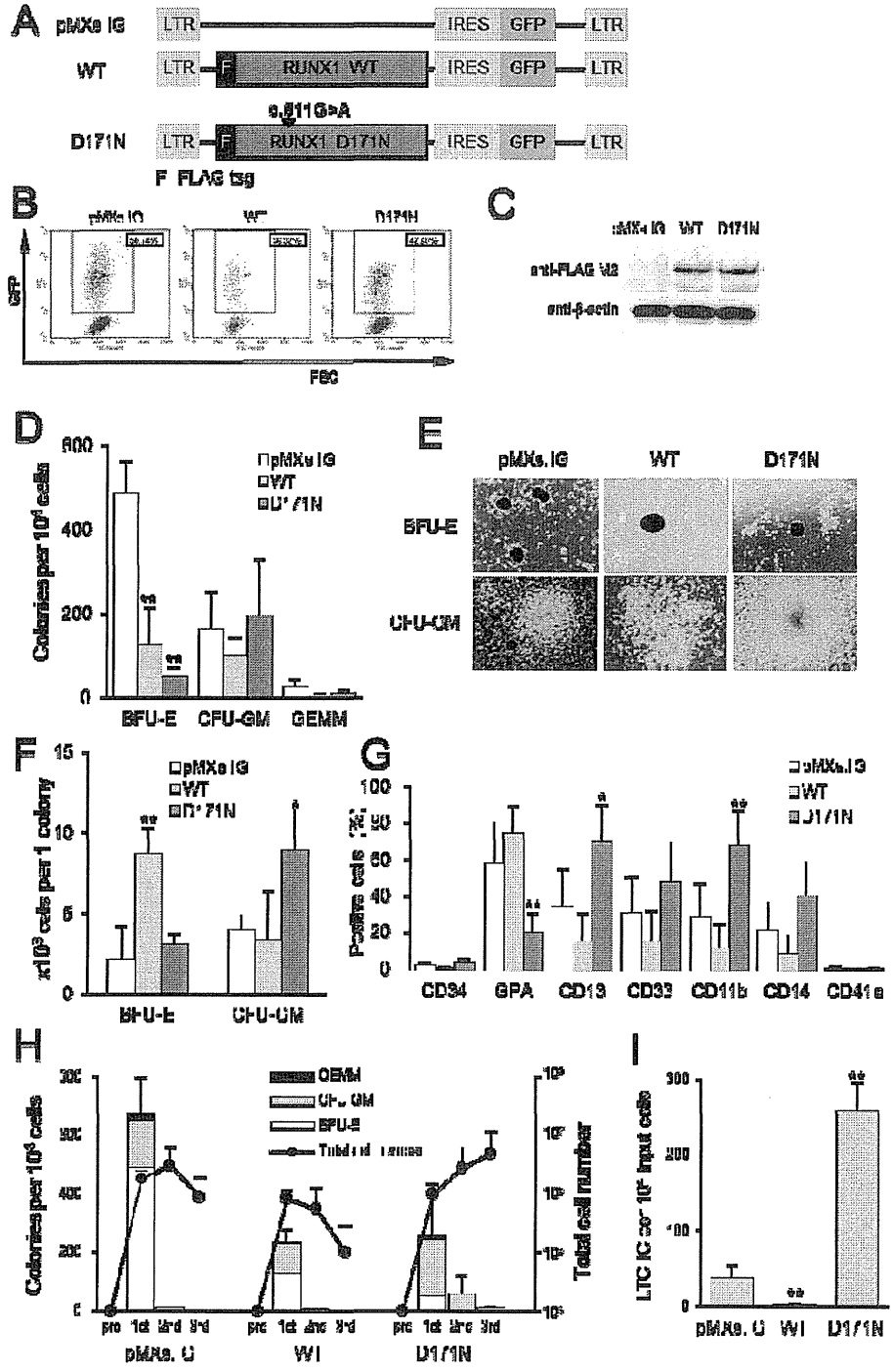

Figure 3

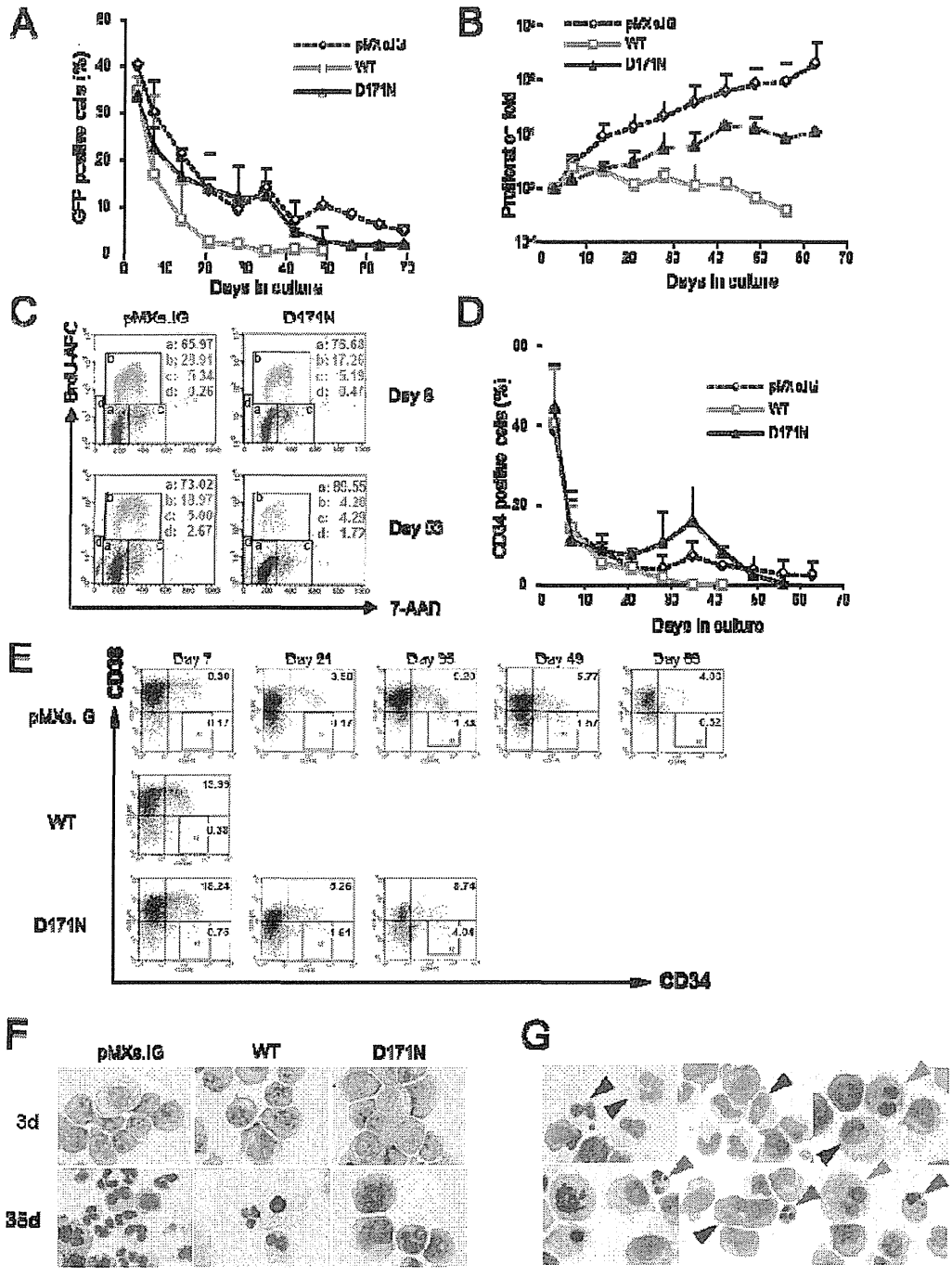

Figure 4

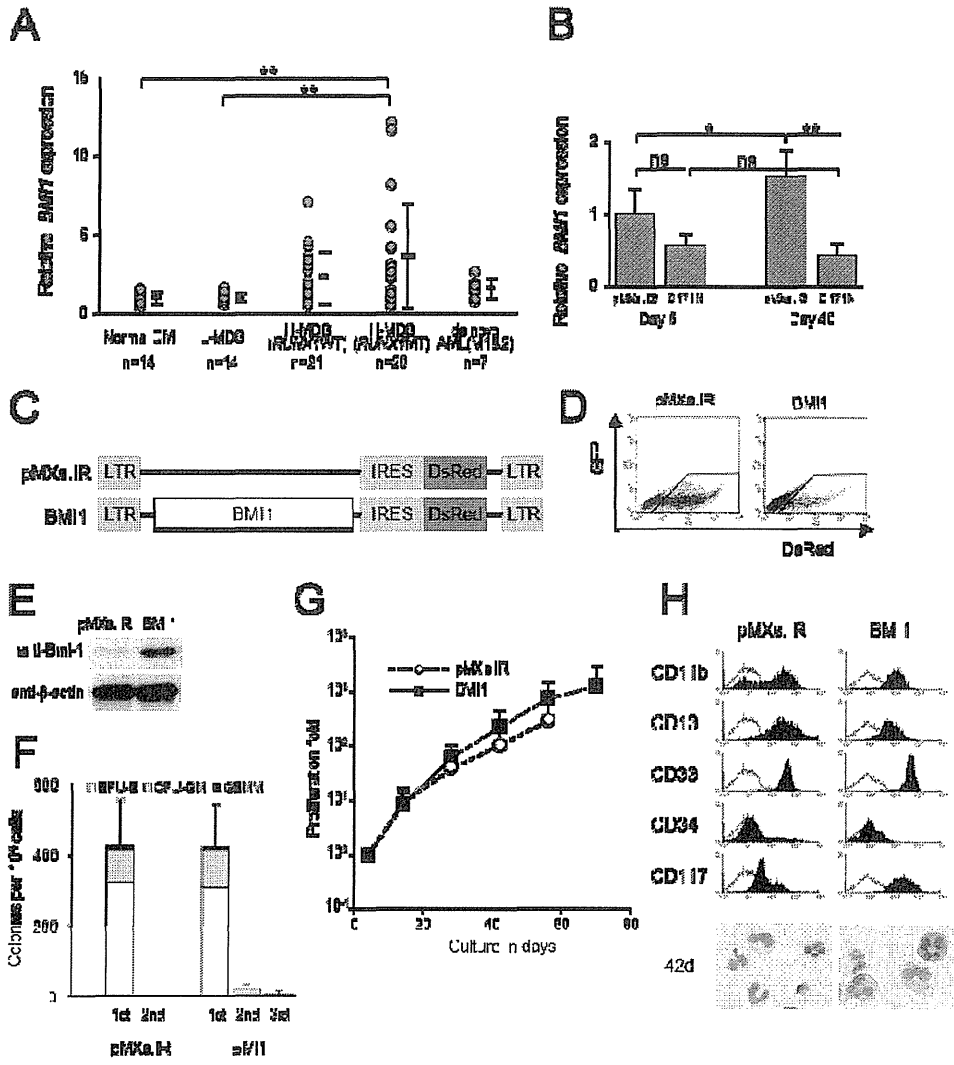

Figure 5

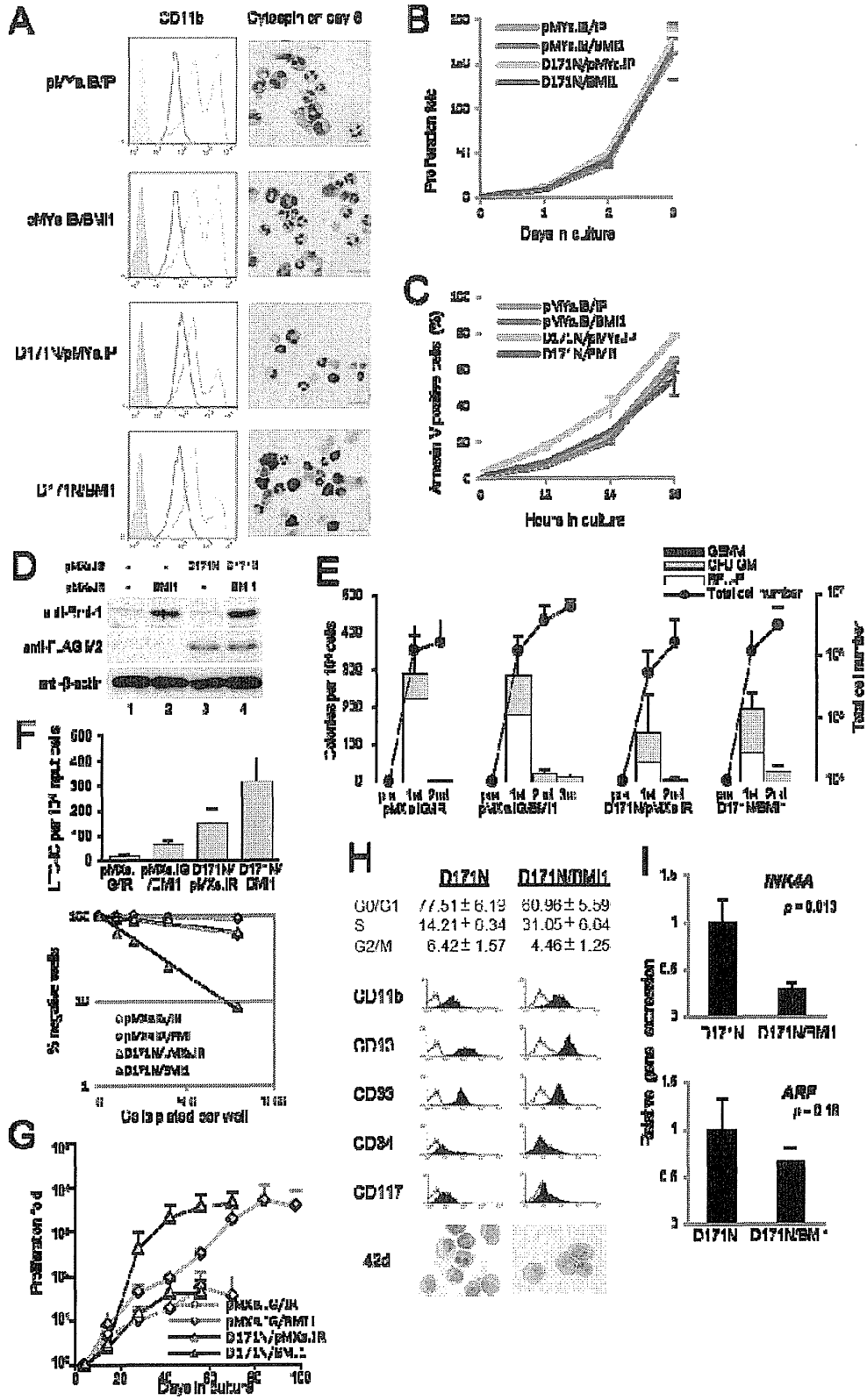

Figure 6